Tensor invariants in resonant Raman scattering on carbon nanotubes

S. Reich and C. Thomsen

Institut für Festkörperphysik, Technische Universität Berlin, Hardenbergstr. 36, 10623 Berlin, Germany, e-mail: `steffi@physik.tu-berlin.de`

Abstract We measured the Raman tensor invariants on single and multiwall nanotubes by linearly and circularly polarized Raman experiments. With the help of recent experiments on aligned nanotubes we obtained the relative intensities of the A_1, E_1, and E_2 phonons in the Raman spectra. Whereas in single-walled tubes Raman scattering is almost exclusively due to A_1 phonons with a strongly uniaxial Raman tensor, the E contributions are around 40% in the multiwall species.

1 Introduction

Raman scattering is widely used to study the physical properties of carbon nanotubes and to characterize nanotube samples. Despite some success to explain, e.g., the Raman spectra of the low-energy modes ($\approx 200\,\mathrm{cm}^{-1}$) or the dependence of the high-energy spectra ($1500-1600\,\mathrm{cm}^{-1}$) on excitation energy, the exact origin of the experimentally observed spectra is still poorly understood. In particular, a convincing interpretation of the high-energy Raman modes and an assignment to the eigenvectors of A_1, E_1, and E_2 symmetry expected in this energy range is still missing. A number of Raman experiments were published, recently, trying to clarify the symmetries of the Raman active phonons in single and multiwall carbon nanotubes.[1–4] These studies were carried out on aligned nanotubes or even single nanotubes. In backscattering perpendicular to the tube axis the possible scattering geometries allow to distinguish between $A_1(zz)$, $A_1(xx)+E_2$, and E_1 symmetry components.

In this paper we show how to obtain the independent elements of the Raman scattering tensors and hence the scattering intensities of the A_1, E_1, and E_2 modes by combining the results of Raman experiments on unoriented and aligned nanotube samples. The Raman spectra show a superposition of A_1 and E modes and do not originate from distinct peaks with different symmetry.

2 Tensor invariants

The Raman tensor like every second rank tensor can be decomposed into three irreducible tensors, the tensor invariants being[5] the isotropic part

$$\bar{\alpha}^2 = \tfrac{1}{9}(\alpha_{xx}+\alpha_{yy}+\alpha_{zz})^2, \tag{1}$$

the symmetric anisotropy

$$\gamma_s^2 = \tfrac{1}{2}[(\alpha_{xx}-\alpha_{yy})^2+(\alpha_{yy}-\alpha_{zz})^2+(\alpha_{zz}-\alpha_{xx})^2]+ \tfrac{3}{4}[(\alpha_{xy}+\alpha_{yx})^2+(\alpha_{xz}+\alpha_{zx})^2+(\alpha_{yz}+\alpha_{zy})^2], \tag{2}$$

and the antisymmetric anisotropy

$$\gamma_{as}^2 = \tfrac{3}{4}[(\alpha_{xy}-\alpha_{yx})^2+(\alpha_{xz}-\alpha_{zx})^2+(\alpha_{yz}-\alpha_{zy})^2], \tag{3}$$

where α_{ij} $(i,j = x,y,z)$ are the elements of the Raman matrix. To some extent, the symmetry of the Raman modes can be deduced by knowing the tensor invariants. E.g., A_1 is the only representation with a non-vanishing $\bar{\alpha}^2$ invariant, while a dominant γ_s^2 contribution is typical for E_1 and E_2 symmetry. Note that E_1 modes can have $\gamma_{as}^2 \neq 0$. Antisymmetric scattering by phonons (E_1 and A_2 symmetry) is forbidden in non-resonant Raman scattering, but might evolve under resonances.[5] In single and multiwall nanotubes antisymmetric contributions are currently controversial; whereas they were reported by Rao *et al.* in multiwall and Duesberg *et al.* in metallic single-walled tubes,[2,4] these results were not confirmed by other groups.[3,6] In semiconducting nanotubes only symmetric Raman tensors were observed in two investigations.[6,7]

3 Experiments

The tensor invariants given in Eq. (1)-(3) are measured on unoriented tubes by linearly and circularly polarized Raman scattering. The setup for the experiments is depicted in the inset of Fig. 1. The polarization direction of the laser light is chosen by the Fresnel rhomb. The laser then passes a $\lambda/4$ zero-order wave plate and is focused (L) onto the sample (S). The scattered light comes back through the $\lambda/4$ plate, is analyzed with a polarization filter (P), and focused onto the entrance slits of a triple-grating monochromator equipped with a CCD detector. By rotating the Fresnel rhomb and the $\lambda/4$ wave plate the spectra in parallel, crossed, corotating, and contrarotating polarization may be recorded without change in the illumination level or spectrometer sensitivity.[5] The tensor invariants are straightforwardly obtained from these four intensities as given in Ref. [5–7]. Raman spectra were excited with the 488 and 647 nm lines of an Ar/Kr laser.

4 Results and Discussion

In Fig. 1 we show the high-energy Raman spectra of semiconducting (a) and metallic (b) single-walled nanotubes. As can be seen in the figure the spectral shape is independent of the polarization, only the overall intensity scales, i.e., the phonons exhibit the same selection rules. The tensor invariants of the high-energy modes in single and multiwall nanotubes and graphite which we obtained from our measurements are given in Tab. 1. Only two of the experimentally observed modes are listed for metallic and semiconducting single-walled tubes; the results for the other modes are very similar. The values given in the last two columns of Tab. 1 are the experimental error ΔI and the ratio between the symmetric anisotropy and the isotropic invariant $\gamma_s^2/\bar{\alpha}^2$. The tensor invariants we measured on the graphite E_{2g} mode agree well with the expected values for a traceless symmetric representa-

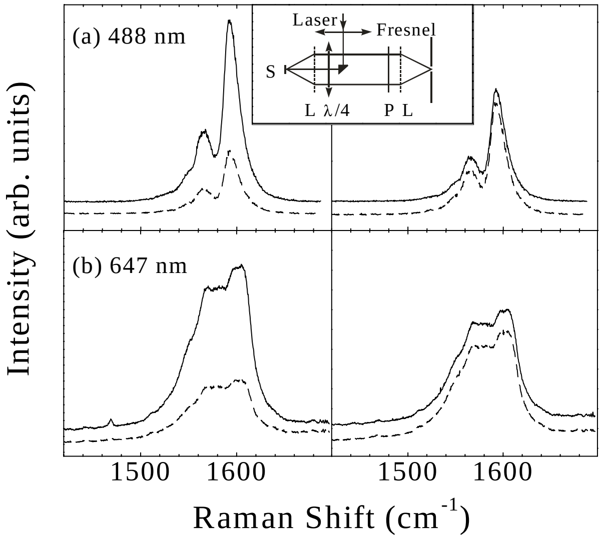

Fig. 1 (a) Raman spectra of semiconducting nanotubes excited with 488 nm; the spectra are shifted for clarity. Left – linear parallel (full lines) and crossed (dashed) polarization; right – corotating (full lines) and contrarotating (dashed) polarization. (b) Same as a but for metallic nanotubes. The inset shows the experimental setup.

tion: The isotropic and the antisymmetric invariants are zero within the experimental error and $\gamma_s^2/\bar{\alpha}^2 = 170$ is large.

The ratio $\gamma_s^2/\bar{\alpha}^2 \approx 9$ in single-walled tubes is close to the expected value of a uniaxial, purely z polarized ($\alpha_{xx} = \alpha_{yy} = 0$) A_1 Raman tensor. In multiwall tubes this ratio is higher suggesting a stronger contribution by E symmetry phonons. On aligned nanotubes the intensity in (z, z) scattering configuration is given by $I(z, z) = \alpha_{zz}^2(A_1)$, in crossed polarization perpendicular to the tube $I(xy, z) = \alpha_{xz}^2(E_1)$, and $I(xy, xy) = \alpha_{xx}^2(A_1) + \alpha_{xx}^2(E_2)$, where we integrated over the (xy) plane, used the measured $\gamma_{as}^2 = 0$ and the identities of the α_{ij} which are given by symmetry. Combining the intensities reported in Ref. [1–3] with the measured $\gamma_s^2/\bar{\alpha}^2$ the relative scattering intensities of the A_1, E_1, and E_2 modes are straightforwardly obtained;[7] they are given in Tab. 2. The by far strongest contribution to the Raman scattering intensity in single and multiwall nanotubes comes from the zz component of the fully symmetric modes. Under resonance the Raman matrix element is determined by the optical transition probability between real electronic states and the electron-phonon matrix element. Thus the strong Raman intensity directly reflects the high transition probability for z polarized light.[8,3] Based on their optical measurements Gommans *et al.* analyzed the metallic Raman spectra assuming that the zz matrix element is the only non-vanishing component and found good agreement if they introduced a small misalignment of the individual tubes.[3] In this context, a surprising result is the vanishing xx intensity of the A_1 modes which is even lower than the obtained E intensities. Because a low absorption and emission probability in the resonant process similarly surpresses the E as the $A_1(xx)$ matrix elements, this probably suggests a small electron-phonon interaction. Compared to single-walled tubes the scattering by E symmetry modes is 1.5 times stronger in multiwall nanotubes. In contrast to A_1 phonons, E modes couple bands of the same symmetry. Since the difference between the electronic singularities scales as $1/d$ the E resonant enhancement is weaker for smaller diameters. Moreover, as d approaches infinity all Raman intensity must be transferred to E_2 symmetry scattering, which is the symmetry of the graphite optical modes.

Table 1 Measured tensor invariants in arbitrary units. Quantities comparable to the experimental error ΔI can be considered zero.

Frequency (cm^{-1})		$45\bar{\alpha}^2$	$6\gamma_s^2$	$5\gamma_{as}^2$	ΔI	$\gamma_s^2/\bar{\alpha}^2$
SWNT	1594	204	252	3	50	9.3
(488 nm)	1565	64	80	1.5	20	9.3
SWNT	1580	50	68	-0.5	2	10.0
(647 nm)	1567	25	66	-0.4	7	10.9
MWNT	1581	2.5	5.8	0.8	0.5	17.2
graphite	1582 (E_{2g})	0.72	16.3	0.4	1	170

Table 2 Relative intensities of the phonon modes in single and multiwall carbon nanotubes.

	$A_1(zz)$	$A_1(xx)$	E_1	E_2
SWNT (semiconducting)	0.7	< 0.05	0.17	0.10
SWNT (metallic)	0.7	< 0.05	0.11	0.14
MWNT	0.6	< 0.05	0.2	0.2

5 Conclusion

In conclusion we studied the Raman intensities of the A_1, E_1, and E_2 symmetry modes in single and multiwall nanotubes. We find that 60-70% of the total scattering intensity originates from the zz Raman matrix element of the fully symmetric modes. This directly reflects the low absorption for light polarized perpendicular to the nanotube axis and can only be explained by considering resonant Raman scattering. The lower E symmetry contribution in single-walled nanotubes as compared to multiwall tubes can similarly be understood by the larger separation between the electronic states and hence weaker resonances.

References

1. H. Sun, Z. Tang, J. Chen, and G.Li, Solid State Commun. **109**, (1999) 365.
2. A. M. Rao, A. Jorio, M. A. Pimenta, M. S. S. Dantas, R. Saito, G. Dresselhaus, and M. S. Dresselhaus, Phys. Rev. Lett. **84**, (2000) 1820.
3. H. H. Gommans, J. W. Alldredge, H. Tashiro, J. Park, J. Magnuson, and A. G. Rinzler, J. Appl. Phys. **88**, (2000) 2509.
4. G. S. Duesberg, I. Loa, M. Burghard, K. Syassen, and S. Roth, Phys. Rev. Lett. (2000), submitted.
5. J. Nestor and T. G. Spiro, J. of Raman Spectroscopy **1**, (1973) 539.
6. S. Reich and C. Thomsen, Phys. Rev. Lett. (2000), in print.
   A. M. Rao, A. Jorio, M. A. Pimenta, M. S. S. Dantas, R. Saito, G. Dresselhaus, and M. S. Dresselhaus, Phys. Rev. Lett. (2000), in print.
7. S. Reich, C. Thomsen, G. S. Duesberg, and S. Roth, Phys. Rev. B (2000), submitted.
8. H. Ajiki and T. Ando, Jpn. J. Appl. Phys. **Suppl. 34-1**, (1994) 107.